
Article:
Fitzgerald, SP orcid.org/0000-0003-2865-3057 (2018) Structure and dynamics of crowdion defects in bcc metals. Journal of Micromechanics and Molecular Physics, 3 (03n04). ARTN 1840003. ISSN 2424-9130

https://doi.org/10.1142/S2424913018400039

Journal of Micromechanics and Molecular Physics

Structure and dynamics of crowdion defects in bcc metals

SP Fitzgerald*
Department of Applied Mathematics
University of Leeds, Leeds, UK

Received date
Accepted date

Abstract
Crowdion defects are produced in body centred cubic metals under irradiation. Their structure and diffusive dynamics play a governing role in microstructural evolution, and hence the mechanical properties of nuclear materials. In this paper we apply the analytical Frenkel-Kontorova model to crowdions and clusters thereof (prismatic dislocation loops) and show that the Peierls potential in which these defects diffuse is remarkably small (in the micro eV range as compared to the eV range for other defects). We also develop a coarse-grained statistical methodology for simulating these fast-diffusing objects in the context of object kinetic Monte Carlo, which is less vulnerable to the low barrier problem than naïve stochastic simulation.

Keywords Point defects; bcc metals; multiscale modelling.

1. Introduction

Crowdions [Kosevich, 2006] are the most stable configuration of self-interstitial atomic defect in the body-centred-cubic (bcc) transition metals V, Nb, Ta, Cr, Mo and W [Derlet *et al.*, 2007]. They are produced in large quantities under irradiation, and agglomerate into the prismatic dislocation loops that characterize radiation damage. They are distinguished from other defect configurations by their effectively one-dimensional nature (along a close-packed crystal direction; $\langle 111 \rangle$ in bcc metals), and exhibit numerous interesting properties, most notably their extremely low migration barriers (of order meV). In the next section, we review the Frenkel-Kontorova / sine- Gordon model for $\langle 111 \rangle$ crowdions, and then discuss its extension to the more realistic double-sine potential. Then we derive the *Peierls potential*, i.e. the effective potential within which the defect diffuses through the crystal. We then discuss crowdion clusters (aka prismatic interstitial-type dislocation loops), and the profound differences between the Peierls potential experienced by loop and that experienced by isolated crowdions. Finally we consider the 3D diffusion of crowdions, which is characterized by fast, virtually free diffusion along close-packed $\langle 111 \rangle$ directions, separated by occasional stochastic changes to other $\langle 111 \rangle$ directions. We show that the anisotropy of the

*S.P.Fitzgerald@leeds.ac.uk

diffusion can be neglected on timescales larger than the inverse direction-changing rate, and suggest an efficient simulation algorithm.

2. Frenkel-Kontorova model

The Frenkel-Kontorova model was originally developed to treat dislocation lines moving through a "washboard" potential, and it has since found applications in areas as diverse as long Josephson junctions in superconductors and the dynamics of DNA [Braun and Kivshar, 2004]. The starting point is the Lagrangian

$$\begin{aligned}\mathcal{L} &= \sum_{n=-\infty}^{\infty}\left\{\frac{m\dot{z}_n^2}{2}-\frac{\beta}{2}\left(z_{n+1}-z_n-a\right)^2-V(z_n)\right\},\\ &\to\int_{-\infty}^{\infty}\left\{\frac{m}{2}\left(\frac{\partial u}{\partial t}\right)^2-\frac{\beta a^2}{2}\left(\frac{\partial u}{\partial z}\right)^2-V\left(u(z,t)\right)\right\}\mathrm{d}z,\end{aligned} \tag{1}$$

where the sum runs over the close-packed string containing one additional atom, which have mass m, position z_n, and are connected by harmonic springs with constant β. The interaction with the surrounding "perfect" lattice is encoded in the periodic potential $V(z_n)$. Assuming the atomic displacement $u_n \equiv z_n - na$ varies slowly with the atomic index n, it can be described by a continuous function $u(z,t)$, with boundary conditions $u(-\infty) = a, u(\infty) = 0$, corresponding to the single additional atom in the string. a is the equilibrium spacing, and is given by $r_0\sqrt{3}/2$ for the $\langle 111\rangle$ direction in a bcc crystal with lattice constant r_0. The simplest choice for the lattice potential is $V_0\sin^2(\pi z/a)$, and if we seek a static solution to the Euler-Lagrange equation corresponding to Eq.(1), we find

$$u(z;z_0) = \frac{2a}{\pi}\tan^{-1}\mathrm{e}^{-\mu(z-z_0)}, \tag{2}$$

where $\mu^2 = 2\pi^2 V_0/\beta a^4$. This displacement profile smoothly varies from 0 to a as z goes from $-\infty$ to ∞, with the variation taking place over a lengthscale $1/\mu$. Thus μ encodes the width of the crowdion, reflecting the relative strengths of the intra-string (β) and surrounding lattice (V_0) interactions. z_0 is the crowdion centre-of-mass coordinate, i.e. its position in the $\langle 111\rangle$ string.

In the continuum limit, the energy of a static crowdion can be calculated by inserting the displacement profile Eq.2 into the (static) Hamiltonian [Kosevich, 2006]

$$E_0 = \int_{-\infty}^{\infty}\left\{\frac{\beta a^2}{2}\left(\frac{\partial u}{\partial z}\right)^2+V\left(u(z,t)\right)\right\}\mathrm{d}z = \left(\frac{\beta a^4\mu^2}{2\pi^2}+V_0\right)\frac{2}{a\mu} = \frac{2a}{\pi}\sqrt{2V_0\beta}. \tag{3}$$

Note how the two terms in the energy, corresponding to the intra-string (β) and surrounding lattice (V_0) interactions, are equal at every point. Also, E_0 is independent of z_0, and so is independent of position. This is an artefact of the continuum limit we have taken, and discreteness can be approximately reintroduced by assuming the crowdion's profile remains fixed as it moves through the crystal, and exploiting the equipartition of the energy between

string and lattice to write

$$E_{\rm discrete} = \sum_{n=-\infty}^{\infty} \left(\frac{\beta}{2} \left(z_{n+1} - z_n - a \right)^2 + V(z_n) \right) \rightarrow 2 \sum_{n=-\infty}^{\infty} V(u_n);\ u_n = u(na), \tag{4}$$

i.e. the continuum solution is evaluated at each discrete atom. The Poisson summation formula then leads to a Fourier series for the *Peierls potential* for the defect:

$$E = E_0 + \frac{2V_0\pi^2}{\mu^2 a^2} \sum_{n=1}^{\infty} n \cos \frac{2\pi n z_0}{a} \ {\rm cosech} \frac{\pi^2 n}{\mu a}. \tag{5}$$

This is the potential in which the defect moves, and the ${\rm cosech}(\pi^2 n/\mu a)$ factor strongly suppresses its magnitude when $\mu a < 1$, which is the case for crowdions. This is delocalization: the intra-string interaction is greater than the lattice interaction, meaning the displacement is spread over many atoms. Moving the defect centre-of-mass one lattice parameter corresponds to tiny motions of many atoms, leading to a suppressed migration barrier. The first term in the series is adequate, and the magnitude of the migration barrier $E_{\rm mig} = E_{\rm max} - E_{\rm min}$ is given to this approximation by

$$E_{\rm mig} \approx \frac{8V_0\pi^2}{\mu^2 a^2} {\rm cosech} \frac{\pi^2}{\mu a}, \tag{6}$$

which is in the μeV range for reasonable values of the parameters (see [Fitzgerald and Nguyen-Manh, 2008] $V_0 \sim$ 1eV, $\beta a^2 \sim$ 50-100 eV).

3. Double sine-Gordon model

Atomistic simulations [Derlet *et al.*, 2007] suggest that, whilst very low, the crowdion migration barrier is in the meV rather than μeV range, indicating that the model described above is not the whole story. In fact, the assumption that the lattice potential is sinusoidal is not always accurate, as density functional calculations show. Particularly for the group VI metals Cr, Mo and W, the potential shows a local minimum midway between the main a-period minima, as can be seen in Fig. 2, [Fitzgerald and Nguyen-Manh, 2008].

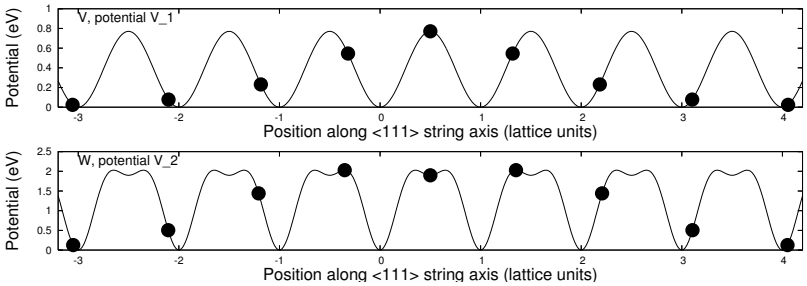

Fig. 1. Atomic positions for crowdions in the single- (top) and double-sine (bottom) models. Parameters are for vanadium and tungsten respectively.

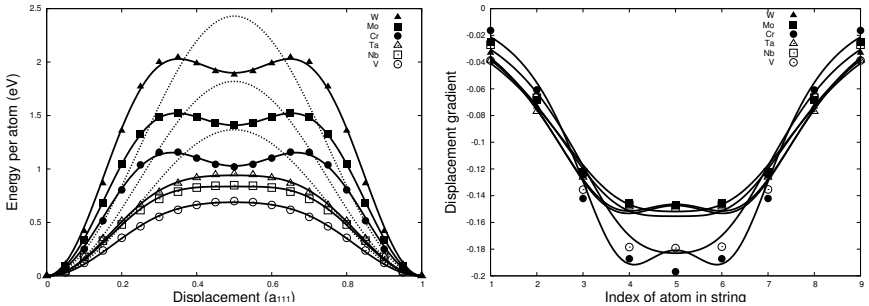

Fig. 2. Lattice potential (left) and atomic displacement gradients (right) for crowdions in the bcc transition metals (DFT; data from [Fitzgerald and Nguyen-Manh, 2008]). Solid lines: double sine fits; dashed line: single sine fit.

These curves can be well-fitted by a double-sine potential

$$V(z) = V_0 \left(\sin^2 \left(\frac{\pi z}{a} \right) + \frac{\alpha^2 - 1}{4} \sin^2 \left(\frac{2\pi z}{a} \right) \right), \tag{7}$$

and the analysis carries forward, leading to a displacement solution

$$u(z; z_0) = \frac{a}{\pi} \arctan \left[\frac{\alpha}{\sinh \left(\mu\alpha(z - z_0) \right)} \right], \tag{8}$$

and the width of the crowdion is now encoded by the combination $\mu\alpha$. A similar, yet more involved, calculation yields the Peierls potential

$$E(z_0) = E_0 + \sum_{j=1}^{\infty} I_j \cos \left(\frac{2\pi j z_0}{a} \right), \tag{9}$$

where

$$I_j = \frac{2V_0\alpha\pi}{\mu a} \mathrm{cosech} \left(\frac{\xi\pi}{2} \right) \times \left\{ \xi \cos \left(\frac{\xi}{4} \ln \frac{q_+}{q_-} \right) - \frac{1}{\alpha\sqrt{\alpha^2 - 1}} \sin \left(\frac{\xi}{4} \ln \frac{q_+}{q_-} \right) \right\}, \tag{10}$$

and $\xi = 2\pi j / \alpha\mu a$ and $q_{+,-} = 1 - 2\alpha^2 \pm 2\alpha\sqrt{\alpha^2 - 1}$. The input parameters can be determined from density functional calculations, and the results for the migration barrier heights for V, Nb, Ta are $6.8 \times 10^{-4}, 0.25 \times 10^{-4}$ and 0.087×10^{-4} eV respectively, and those for Cr, Mo, W are $12 \times 10^{-3}, 2.4 \times 10^{-3}$ and 2.6×10^{-3} eV respectively. A clear group-specific trend emerges, with the group VI metals having a deeper local minimum, and hence a larger migration barrier, than their group V counterparts. Still, all these barriers are remarkably low. In a crowdion cluster, the magnitude of the lattice potential experienced by a defected string depends on how many of its neighbours are undefected, as we discuss below.

Most defects migrate stochastically through the crystal with a diffusivity D that takes the form $D = D_0 \exp(E_{\mathrm{mig}}/k_{\mathrm{B}}T)$, corresponding to hops through the lattice that occur with an Arrhenius rate proportional to $\exp(E_{\mathrm{mig}}/k_{\mathrm{B}}T)$ (T is the temperature, E_{mig} is the

migration barrier and k_{B} is Boltzmann's constant). This expression depends on the implicit assumption that $E_{\mathrm{mig}} \gg k_{\mathrm{B}}T$, i.e. the hops are rare events. This clearly does not apply to crowdions for all but cryogenic temperatures. Indeed, for $E_{\mathrm{mig}} \ll k_{\mathrm{B}}T$, the diffusion is effectively free, and the diffusivity grows linearly with temperature. For 1D motion in a sinusoidal potential, an exact solution for the hop rate exists for all temperatures, see e.g. [Swinburne *et al.*, 2013].

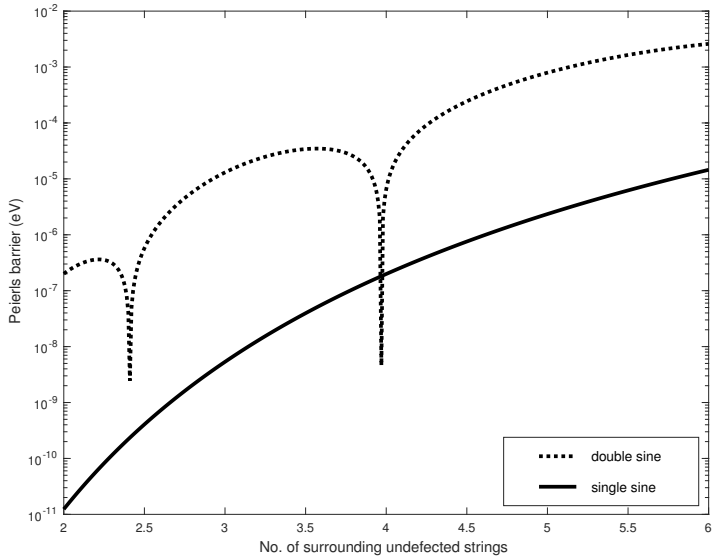

Fig. 3. Effect of number of undefected neighbour strings on crowdion Peierls barriers $E_{\mathrm{mig}} = E_{\mathrm{max}} - E_{\mathrm{min}}$ given by Eqs. (6) and (10). An isolated crowdion has 6, whereas most boundary crowdions in a cluster have 2.

4. Multi-crowdion solutions

Crowdions cluster together to form $\boldsymbol{b} = \frac{1}{2}\langle 111\rangle$ prismatic dislocation loops, and the Frenkel-Kontorova model can be extended to treat these clusters [Dudarev, 2003]. Using the single-sine form for simplicity, the interaction potential between two crowdions in neighbouring parallel $\langle 111\rangle$ strings with displacement fields $u_0 = u(z;0), u_1 = u(z;x)$ can be written

$$\begin{aligned} E_{\mathrm{int}}(x) &= \int_{-\infty}^{\infty} \frac{V_0}{6} \sin^2\left(\frac{\pi}{a}\left(u_0 - u_1\right)\right) \mathrm{d}z \\ &= \frac{2V_0}{3\mu} \tanh\frac{\mu x}{2}\left(\frac{\mu x}{2}\mathrm{sech}^2\frac{\mu x}{2} + \tanh\frac{\mu x}{2}\right), \end{aligned} \tag{11}$$

where x is the separation between the crowdions' centres of mass. This assumes that the profile of the crowdions, encoded by μ, does not change as they interact. A more detailed calculation [Fitzgerald, 2015] shows that this does not affect the results. The factor of $1/6$ arises because V_0 was defined as the lattice potential for an isolated crowdion, surrounded by 6 neighbours. Each member of a crowdion pair has 5 undefected neighbour strings, so its $\mu \to \sqrt{5/6}\mu$ compared to an isolated crowdion.This small correction has important effects due to the extreme nonlinearity of the Peierls potentials given in Eqs.(6) and (10). For tungsten, the 2-crowdion interaction potential above is a slight (maximum 0.3eV) repulsion for large distances, and an attractive well when the separation is less than about 12 atomic spacings. The well depth is $\sim$3eV (DFT gives somewhat less than this [Marinica *et al.*, 2013], but the agreement for the single sine model is reasonable), so crowdions bind strongly together. The consequence for their displacement profile is that their μ is reduced, and hence they are more spread out down the $\langle 111 \rangle$ string. For large clusters, only crowdions near the edge experience strong interactions with the undefected lattice. Crowdions in the interior are delocalized to such an extent that they are indistinguishable from perfect lattice, and the cluster becomes a prismatic dislocation loop, with strain localized to the perimeter. At the perimeter, each boundary crowdion has 2 or 3 undefected neighbour strings (depending on the geometry of the loop – small $\boldsymbol{b} = \frac{1}{2}\langle 111 \rangle$ loops are typically hexagonal, so "corner" crowdions have 3 perfect neighbours, whilst "edge" crowdions have 2). Fig.3 shows the effect this has on the Peierls potential for crowdions in tungsten. The enhanced delocalization reduces the Peierls potential by at least 4 orders of magnitude, rendering it zero to all intents and purposes. This suppression comes again from the cosech$(.../\mu)$ term, which is an extremely nonlinear function of μ. This completely outweighs the increased number of boundary crowdions experiencing the Peierls potential[a] therefore prismatic dislocation loops have an energy barrier to migration lower even than isolated crowdions. This does not imply that their diffusivity is greater, but rather that the temperature dependence of the loop diffusivity deviates from the Arrhenius form at an even lower temperature than that of an isolated crowdion. The greater number of degrees of freedom in a loop mean that the the diffusivity is reduced.[b]

5. 3D diffusion of single crowdions

Molecular dynamics simulations [Derlet *et al.*, 2007] confirm the fast 1D nature of crowdion migration, but also show the defects changing from one $\langle 111 \rangle$ direction to another. This occurs at a slower rate, comparable to the "rare event" hops of other crystal defects. This allows the crowdion to explore the entirety of the crystal, and in this section we calculate the effect on 3D diffusion, and outline a Monte Carlo algorithm for its simulation.

Firstly assume that the direction-changing transition is a Poisson process with rate Γ. Then the time intervals between changes of direction will be exponentially distributed,

[a]Loops would need to contain several million defects to have the $>$10,000 boundary crowdions required.

[b]This can be seen by considering the normal modes of the perimeter crowdions which interact with the surrounding lattice: only the "centre-of-mass" degree of freedom translates the cluster, with the rest of the fluctuations corresponding to internal configuration changes.

with pdf $\psi(t) = \Gamma \exp(-\Gamma t)$. If we further assume that, during the time interval t spent between direction changes, the crowdion diffuses normally with diffusivity D, then the hop lengths x, conditioned on the time interval t, will have the normal distribution $\Lambda(x|t) = \exp(-x^2/2Dt)/\sqrt{2\pi Dt}$. Since the hops are independent, we can reorder the series of hops, treat each $\langle 111 \rangle$ direction independently in 1D, and project onto 3D space at the end. The fact that the directions along which the crowdion can diffuse are linearly dependent is immaterial, as shown below. This analysis can be similarly applied to any crystal structure.

In the bcc lattice, there are four (unsigned) $\langle 111 \rangle$ directions along which crowdions can move, with unit vectors $\hat{\boldsymbol{e}}_{\mathbf{1,2,3,4}}$. The final position of the crowdion is $\boldsymbol{x_f} = \sum_{i=1}^{4} s_i \hat{\boldsymbol{e}}_{\boldsymbol{i}}$, where s_i is the sum of the signed hop lengths in the i direction. Each of these hop lengths is normally distributed with zero mean and variance $D\Delta t$ (and the Δts are exponentially distributed, though that is not required). The total time $t = \sum_{i=1}^{4} t_i$ where t_i is the time spent hopping in each direction, i.e. the sum of the Δts for each direction. The expected value for $|\boldsymbol{x_f}|^2$ is given by

$$\begin{aligned} \mathbb{E}\left(|\boldsymbol{x_f}|^2\right) = \mathbb{E}\left(\sum_{i=1}^{4} s_i \hat{\boldsymbol{e}}_{\boldsymbol{i}}\right)^2 &= |\hat{\boldsymbol{e}}_{\boldsymbol{i}}|^2 \mathbb{E}\left(s_1^2\right) + \ldots + 2\hat{\boldsymbol{e}}_{\mathbf{1}} \cdot \hat{\boldsymbol{e}}_{\mathbf{2}} \mathbb{E}(s_1 s_2) + \ldots \\ &= Dt_1 + Dt_2 + Dt_3 + Dt_4 + 0 \\ &= Dt, \end{aligned} \tag{12}$$

where in the second line we used the fact that variances add in sums of normally distributed random variables, and that $\mathbb{E}(s_1 s_2) = \mathbb{E}(s_1)\mathbb{E}(s_2) = 0$ by independence. The $\hat{\boldsymbol{e}}_{\boldsymbol{i}}$s need not be orthogonal.

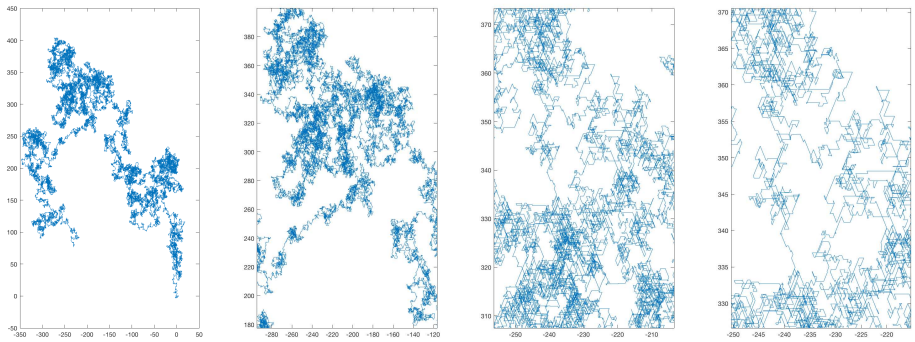

Fig. 4. Left to right: increasing magnification views of an example trajectory from crowdion Monte Carlo. Only at the smallest scales is the anisotropy of the diffusion evident. The time t spent on a particular $\langle 111 \rangle$ direction is drawn from an exponential distribution, then the distance diffused on that direction prior to the change is drawn from a normal distribution with variance Dt.

With the above assumptions, the pdf W for the crowdion position x at time t satisfies

the Chapman-Kolmogorov equation [Montroll and Lebowitz, 1987]

$$W(x,t) = \int_0^t \int_{-\infty}^{\infty} \psi(t-t')\Lambda(x-x'|t-t')W(x',t')\mathrm{d}x'\mathrm{d}t' + \left(1 - \int_0^t \psi(t)\mathrm{d}t\right) W(x,0). \tag{13}$$

This reflects the sum over all possible hop lengths and times, and the second term is the probability density for the particle remaining at $x = 0$ until time t, $W(x,0) = \delta(x)$. Inserting the above forms for ψ and Λ then taking Fourier transforms in x and Laplace transforms in t, $W(x,t) \to W(k,s)$, leads to

$$W(k,s) = \frac{2s + \Gamma k^2 D}{(s+\Gamma)(2s + k^2 D)}. \tag{14}$$

Now, since

$$\frac{\partial^2 W(k,t)}{\partial k^2} \equiv \int_{-\infty}^{\infty} \mathrm{e}^{ikx}(-x^2)W(x,t)\mathrm{d}x, \tag{15}$$

we can differentiate $W(k,s)$ twice with respect to k and set $k = 0$ to get (minus) the Laplace-transformed expected value for x^2. Inverting the transform gives

$$\langle x^2 \rangle = D\left(t - \frac{1-\exp(-\Gamma t)}{\Gamma}\right) \sim Dt \text{ when } t \gg \frac{1}{\Gamma}. \tag{16}$$

So for sufficiently large times, the effective diffusivity is that of the 1D fast motion, but how long until this approximation is reasonable is controlled by the rate of direction changes, Γ. Indeed, for $t \ll 1/\Gamma$, $\langle x^2 \rangle \sim D\Gamma t^2/2$. The MD simulations of [Derlet *et al.*, 2007] give a rate

$$\Gamma = 6.59 \times 10^{12} \exp(-0.385\,\mathrm{eV}/k_\mathrm{B}T)/\mathrm{sec} \tag{17}$$

for crowdions in tungsten, whereas the migration energy for vacancies is found to be 1.78eV. This suggests that, on the timescale of vacancy diffusion, crowdion diffusion is effectively isotropic, and the 1D nature of hops can be neglected. Crowdion clusters/prismatic loops, on the other hand, stick to single $\langle 111 \rangle$ directions for much longer. Whilst rotations for very small loops are not impossible [Arakawa *et al.*, 2006], the activation energy is much higher.

Stochastic computer simulations are most efficient when the events being sampled have rates as similar as possible. A kinetic Monte Carlo simulation of, say, crowdion and vacancy hopping would spend the vast majority of its time moving crowdions since their barriers are so low compared to those for vacancies (this is known generically as the low barrier problem). A more efficient approach would be to sample the direction-changing events, and then draw the crowdion's 1D motion from a normal distribution with appropriate time-dependent variance, as in the analytical approach above. Fig. 4 shows an example trajectory from a million step simulation of this type, which can be performed in under a minute on an ordinary laptop. The 1D $\langle 111 \rangle$ hops are only apparent when 'zoomed in', and at larger scales are indistinguishable from standard diffusion. Indeed, given that crowdions' diffusion rate is typically many orders of magnitude higher than any other species', it may be advantageous to treat the crowdions using a density functional, in analogy with the DFT

treatment of electrons. The approach could be extended to model the nucleation and growth of prismatic loops from a population of crowdions and vacancies formed by a cascade. Here, the 1-D nature of the motion is likely to still play a role, since crowdions in adjacent parallel strings interact via the potential of Eq.(11). Such an approach would maintain full discrete defect resolution, along with spatial distribution information, and as such would by complementary to existing techniques such as stochastic cluster dynamics [Marian and Bulatov, 2011].

6. Conclusions

In this paper, we have derived the surprising result that clusters of crowdions (aka prismatic dislocation loops) can move through a bcc crystal lattice virtually unimpeded (aside from dissipation). The periodic (Peierls) potential in which they move is fractions of a micro eV: several orders of magnitude lower than even that for an isolated crowdion. The reason for this is *delocalization* – the lattice displacement induced by the additional atoms is spread over many atoms, meaning the translation of its centre of mass corresponds to the tiny motions of many more atoms. This is analogous to how the existence of dislocations allows the plastic deformation of crystals at far lower applied stresses than their "theoretical strength" would suggest. We then showed that the highly anisotropic diffusion of crowdions, which atomistic simulations have demonstrated, can be safely neglected at timescales sufficiently far above the timescale for direction changes. This will aid the development of hybrid mesoscale Monte Carlo simulations of defect structure evolution, by avoiding the low barrier problem associated with the suppression of the Peierls potential.

As a one-dimensional analytical approach, the model presented here cannot hope to match the full quantitative accuracy of many-atom techniques such as DFT. Whilst the double-sine form for the lattice potential captures very well the corresponding DFT calculation, the assumption of harmonic nearest-neighbour interactions along the string is a clear idealization. Nevertheless, the model offers insights unavailable to more sophisticated numerical approaches, in particular the explanation of the smallness of the Peierls barriers. As far as the author is aware, these are inaccessible to numerical approaches as the numbers are simply too small. Some quantitative shortcomings could also be overcome by independently adjusting the model parameters to fit values obtained by more precise methods (e.g. the depth of the crowdion-crowdion pair potential could simply be set equal to the DFT value). Moreover, the computational efficiency afforded by this approach allows simulations with individual defect resolution to be extended to length- and time-scales far greater than that available to molecular dynamics.

References

Arakawa, K., Hatanaka, M., Kuramoto, E., Ono, K. and Mori, H. [2006] "Changes in the burgers vector of perfect dislocation loops without contact with the external dislocations," *Physical review letters* **96**(12), 125506.

Braun, O. M. and Kivshar, Y. S. [2004] *The Frenkel-Kontorova model: concepts, methods, and applications* (Springer).

Derlet, P. M., Nguyen-Manh, D. and Dudarev, S. [2007] "Multiscale modeling of crowdion and vacancy defects in body-centered-cubic transition metals," *Physical Review B* **76**(5), 054107.

Dudarev, S. [2003] "Coherent motion of interstitial defects in a crystalline material," *Philosophical Magazine* **83**(31-34), 3577–3597.

Fitzgerald, S. [2015] "Crowdion–solute interactions: Analytical modelling and stochastic simulation," *Nuclear Instruments and Methods in Physics Research Section B: Beam Interactions with Materials and Atoms* **352**, 14–17.

Fitzgerald, S. and Nguyen-Manh, D. [2008] "Peierls potential for crowdions in the bcc transition metals," *Physical review letters* **101**(11), 115504.

Kosevich, A. M. [2006] *The crystal lattice: phonons, solitons, dislocations, superlattices* (John Wiley & Sons).

Marian, J. and Bulatov, V. V. [2011] "Stochastic cluster dynamics method for simulations of multispecies irradiation damage accumulation," *Journal of Nuclear Materials* **415**(1), 84–95.

Marinica, M., Ventelon, L., Gilbert, M., Proville, L., Dudarev, S., Marian, J., Bencteux, G. and Willaime, F. [2013] "Interatomic potentials for modelling radiation defects and dislocations in tungsten," *Journal of Physics: Condensed Matter* **25**(39), 395502.

Montroll, E. W. and Lebowitz, J. L. [1987] *Fluctuation Phenomena* (North-Holland), ISBN 0444870385.

Swinburne, T., Dudarev, S., Fitzgerald, S., Gilbert, M. and Sutton, A. [2013] "Theory and simulation of the diffusion of kinks on dislocations in bcc metals," *Physical Review B* **87**(6), 064108.

Acknowledgments

SPF thanks Dr D Nguyen Manh and Dr M-C Marinica for many helpful discussions. This work was supported in part by the UK EPSRC, Grant number EP/R005974/1.